Magnetochronology and age models of deposition of the Melka Kunture stratigraphic sequence (Upper Awash, Ethiopia) and age assessments of the main archeological levels therein contained

Serena Perini [a, *], Giovanni Muttoni [a], Edoardo Monesi [b, 1], Rita T. Melis [c], Margherita Mussi [d]

[a] Dipartimento di Scienze della Terra 'Ardito Desio', Universita degli Studi di Milano, via Luigi Mangiagalli 34, 20133, Milan, Italy [b] via Mecenate 76, 20138, Milan, Italy [c] Dipartimento di Scienze Chimiche e Geologiche, Universita di Cagliari, Cittadella Universitaria, 09042, Monserrato, Italy [d] Dipartimento di Scienze dell'Antichita, Universita di Roma Sapienza, Piazzale Aldo Moro 5, 00185, Rome, Italy

articleinfo

Article history:
Received 29 June 2021
Received in revised form
27 October 2021
Accepted 28 October 2021
Available online 8 November 2021 Handling

Editor: Dr. Giovanni Zanchetta

Keywords:
Melka Kunture
Ethiopia
Hominins
Magnetostratigraphy
Pleistocene

abstract

We present new magnetostratigraphic results from the Melka Kunture sedimentary sequence outcropping along the Gombore and Garba gullies in the Upper Awash Valley of Ethiopia that provide a new temporal framework for human presence in this area of the Ethiopian plateau in the Pleistocene. We obtained a time-diagnostic sequence of normal and reverse polarity magnetozones representing a relatively continuous magnetochronologic record extending from the Brunhes Chron at the top to the Olduvai Subchron or possibly the Reunion Subchron at the base, assembled from 9 stratigraphic sections correlated in a regional lithostratigraphic context. By integrating our chronology provided by paleomagnetism with $^{40}Ar/^{39}Ar$ dating from the literature, we generated simple yet reliable and testable age models of deposition for the Melka Kunture sedimentary sequence that we used to estimate the mean ages of the main archeological levels therein contained that resulted ranging from ~0.6 Ma to ~2.1 Ma thus representing altogether one of the most persistent and prolonged records of human presence of the entire African continent.

1. Introduction

The archeological area of Melka Kunture (842oN; 3835oE) is located in the Upper Awash Valley of the Ethiopian plateau, about 50 km southwest of Addis Ababa. Here, a relatively continuous stratigraphic sequence mainly comprised of fluvial/alluvial siliciclastic and volcaniclastic deposits variably intercalated with tuff/ cinerite, informally known as Melka Kunture succession (e.g., Bardin et al., 2004; Kieffer et al., 2002, 2004; Raynal et al., 2004; Raynal and Kieffer, 2004; Gallotti and Mussi, 2017), is exposed along a network of gullies incised by tributaries of the Awash River (Fig. 1). Different stratigraphic levels of archeological and paleoanthropological interest have been discovered throughout this sequence in the last decades, spanning from Late Stone Age to Oldowan (Chavaillon et al., 1974; Chavaillon et al., 1979; Chavaillon and Coppens, 1986; Chavaillon and Berthelet, 2004; Chavaillon and Piperno, 2004; Gallotti and Mussi, 2017, 2018; Gallotti et al., 2010; Mussi and Gallotti, 2014; Mussi et al., 2014, 2016).

Previous magnetostratigraphic studies (Westphal et al., 1979; Tamrat et al., 2014), combined with radiometric dating of tuff/cinerite using K/Ar (Schmitt et al.,1977; Chavaillon and Piperno, 2004) and $^{40}Ar/^{39}Ar$ (Morgan et al., 2012), suggested that the Melka Kunture sequence deposited in a magnetochronologic interval spanning from the early Brunhes Chron (<0.773 Mega-annum or Ma; geomagnetic polarity time scale of Channell et al. (2020) used throughout) at the top to the Olduvai Subchron (1.770 Ma to 1.925 Ma) at the base. These valuable magnetostratigraphic data (e.g., Tamrat et al., 2014) are however difficult to integrate in the ever-growing inventory of archeological levels described at Melka Kunture (e.g., Gallotti and Mussi, 2017, 2018) because of the laterally discontinuous nature of the stratigraphic sequence.

The aim of this work is therefore to provide new magnetochronological constraints on the deposition of the Melka Kunture

* Corresponding author.
E-mail address: serena.perini@unimi.it (S. Perini).
[1] Independent author

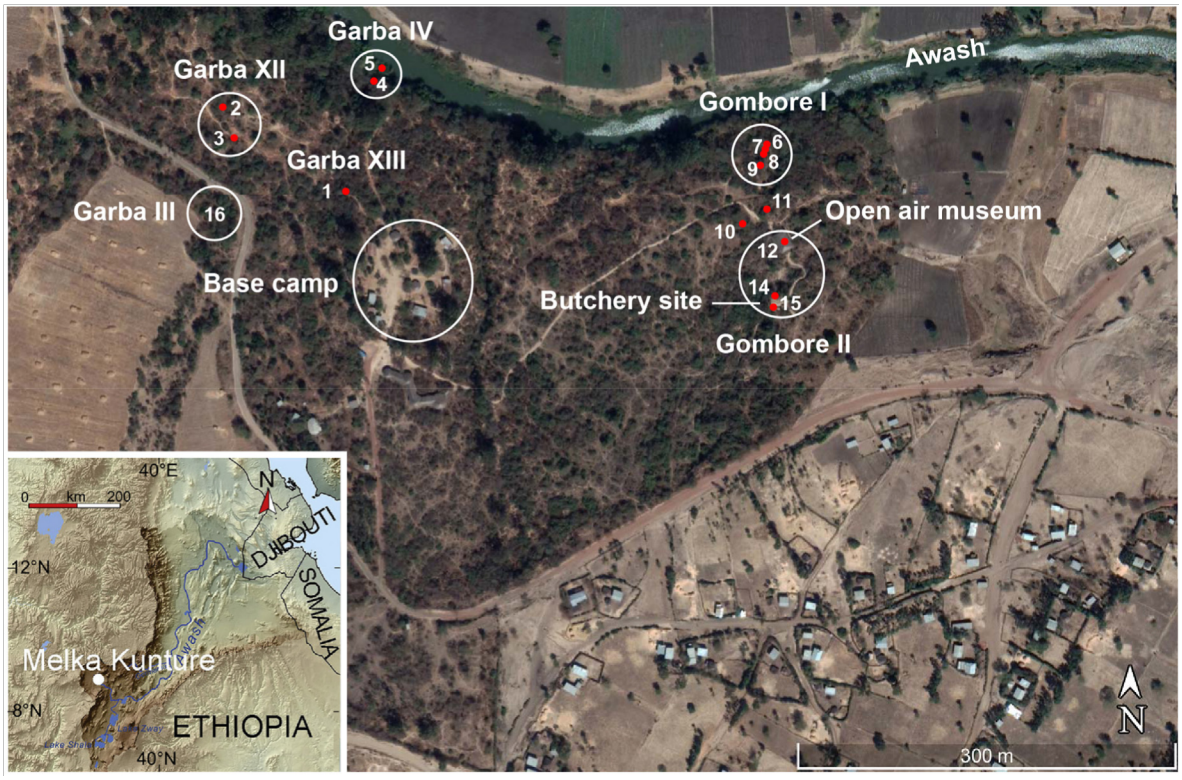

Fig. 1. Google Earth map of the Melka Kunture archeological area in Ethiopia. Gombore and Garba are the main gullies where we studied a total of 9 stratigraphic sections to assess the chronology of deposition of the Melka Kunture sequence and main archeological levels present therein. Numbers refer to georeferenced points reported also in the stratigraphic scheme of Fig. 2.

sedimentary sequence and related archeological levels. Sampling for magnetostratigraphy has been conducted along 9 stratigraphic sections outcropping along two adjacent gullies termed Gombore and Garba (Figs. 1 and 2). In these sections we identified the main archeological levels from the literature including, from younger to older, Gombore II-2 Butchery site, Gombore II Open Air Museum, Gombore Id, Gombore Ig, and Gombore IB for the Gombore gully, and Garba III, Garba XIIJ, Garba IVD, Garba IVE, and Garba IVF for the Garba gully (Fig. 2). Our new magnetostratigraphic data have been integrated with $^{40}Ar/^{39}Ar$ age data from Morgan et al. (2012) in order to generate age models of deposition for the Gombore and Garba gullies sequences and derive (interpolated or extrapolated) best-fit ages of the main archeological levels therein contained.

2. Geological setting

At Gombore gully, we studied, from top to bottom, stratigraphic sections GX, GII2 - G2SAG, GII6, GOAMII, GIISag17I, GXIS, and Gombore I, this latter subdivided into four portions GG, GIG, GIS, and GIC (Fig. 2 and acronyms therein described), while at Garba gully, we studied sections GBIII, GBXIIC - GBXIIB - GBXIIA, GBIVO, and GBIV (Fig. 2). The prevalent lithologies (Fig. 2) are litoquartzarenites and reworked volcanoclastic material, sometimes cross-laminated and often containing lapilli or tuff chips, as well as silts, silty clays, and conglomerates, which are variably intercalated with cinerite and tuff in primary position, some of which have been dated with K/Ar and $^{40}Ar/^{39}Ar$ (Schmitt et al., 1977; Morgan et al., 2012), as well as massive lahar deposits. Altogether, the sedimentary succession deposited in an alluvial/fluvial plain context characterized by occasional but persistent volcanogenic input (see Raynal et al., 2004; Raynal and Kieffer, 2004; Chavaillon, 1979 for further details). These lithologies are particularly favourable for paleomagnetic analyses because of the general presence of finegrained sediments (fine sand, silt), occurring even within the coarsest fractions either as matrix or as individual layers or pockets, as well as for the virtually ubiquitous presence in these sediments of a volcaniclastic fraction enriched in ferromagnetic minerals (as testified by the relatively high remanent magnetization values of the investigated samples; see also below).

In the studied sections (Fig. 2), we identified the following tuff levels provided with what we initially considered acceptable $^{40}Ar/^{39}Ar$ ages (after Morgan et al., 2012), with errors here expressed at 2s level: at Gombore gully, Former D tuff 27e09 at 0.709 ± 0.026 Ma, Tuff 27e08 at 0.875 ± 0.020 Ma (but see below in

Paragraph 4 for the reliability of this datum), Former B tuff 27e12 at 1.200 ± 0.140 Ma, and Tuff 27e03 at 1.393 ± 0.324 Ma, while at Garba gully, Tuff 27e23, informally termed also "Grazia Tuff", at 1.719 ± 0.398 Ma (but see below in Paragraph 4 for the reliability of this datum) (Fig. 2).

As stated in the Introduction, several archeological and/or paleoanthropological levels have been described in this sequence. At Gombore gully (Fig. 2), these include the Gombore II-2 Butchery site, containing Acheulean lithic tools as well as faunal remains and associated ichnological evidence (Altamura et al., 2020; MendezQuintas et al., 2019), Gombore II Open Air Museum, with middle Acheulean lithic tools and remains possibility pertaining to early Homo heidelbergensis (Royer and Coppens, 1975; Profico et al., 2016), Gombore Id and Gombore Ig with additional Acheulean evidence, and Gombore IB with remains of Homo ergaster associated with Early Acheulean lithic tools (Di Vincenzo et al., 2015; Gallotti and Mussi, 2017; Mussi et al., 2021). In the Garba gully sequence (Fig. 2), main archeological levels are Garba IIIC, with an Acheulean lithic industry, above which lies an early Middle Stone Age level that yielded three cranial fragments attributed to archaic Homo

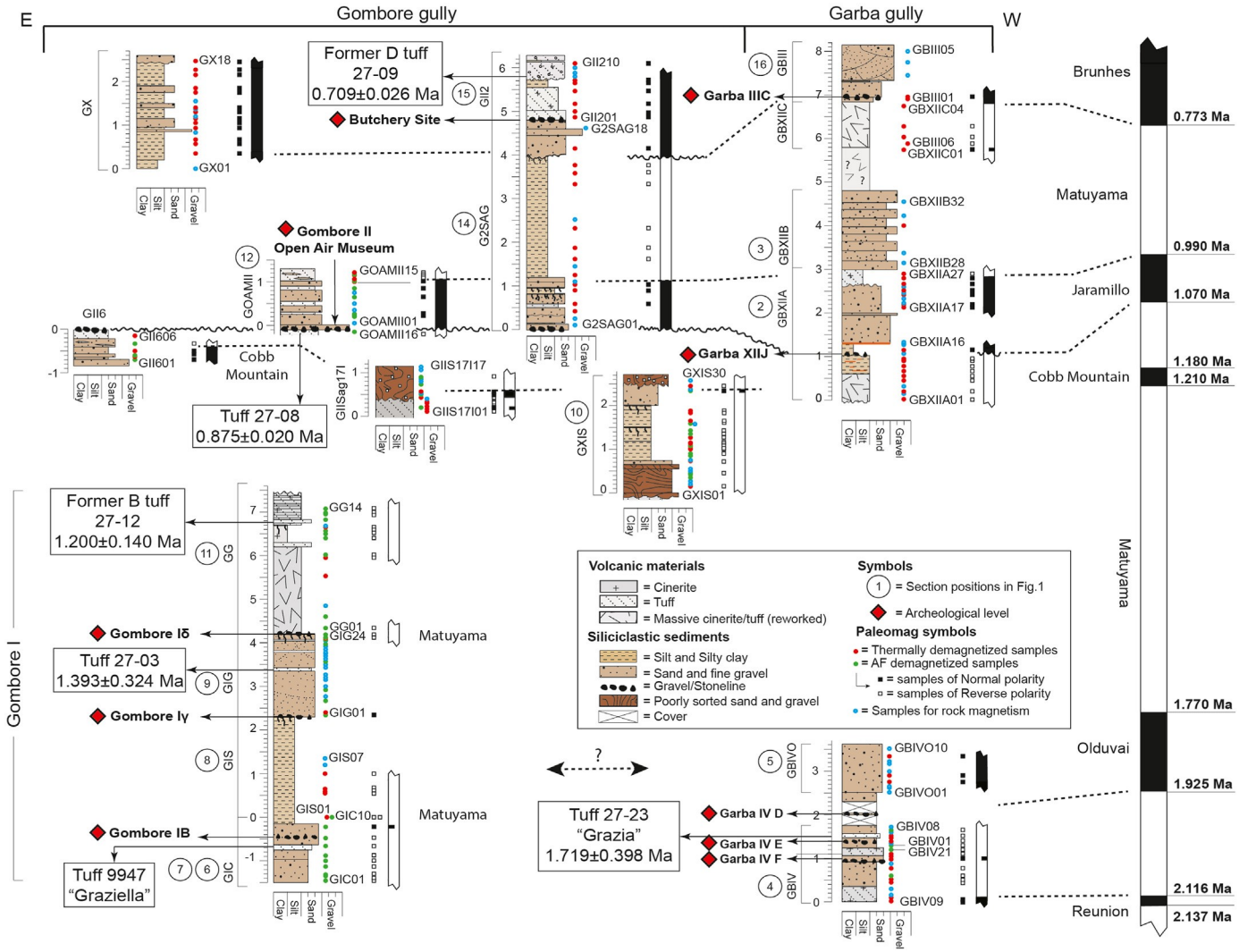

Fig. 2. Stratigraphic scheme of the Melka Kunture sedimentary succession constructed using a total of 9 lithological logs from Gombore and Garba gullies correlated using essentially magnetostratigraphy in conjunction with the available radiometric dating of tuff levels. Circled numbers to the side of the logs refer to georeferenced points in Fig. 1. Samples for paleomagnetic and rock-magnetic analyses are listed next to the logs (see legend for symbols). The characteristic remanent magnetization component (ChRM) vectors extracted from samples that yielded suitable results upon thermal or alternating field (AF) treatment (see legend for symbols) were used to develop a magnetic polarity stratigraphy (white squares for reverse polarity and black squares for normal polarity) that is correlated to the geomagnetic polarity time scale of the Pleistocene with ages from Channell et al. (2020). In the Gombore I log, GIC is Gombore I Sondaggio Chavaillon, GIS is Gombore I Scalinata, GIG is Gombore I Gamma and GG is Gombore I Gully. Other acronyms are as follows:
GIISag17I is Gombore II Saggio 2017 I, GXIS is Gombore XI "Sol", GOAMII is Gombore II Open Air Museum. See text for additional information.

sapiens (Mussi et al., 2014), Garba XIIJ, which yielded Early Acheulean lithic tools and faunal remains (Piperno, 2001; Chavaillon and Berthelet, 2004), Garba IVD, which yielded a rich Early Acheulean assemblage (Gallotti, 2013), Garba IVE, located immediately below the "Grazia Tuff" (tuff 27e23 of Morgan et al., 2012) and containing a partial mandible attributed to Homo erectus (Condemi, 2004; Zilberman et al., 2004a, 2004b; Zanolli et al., 2016) associated with Oldowan lithic artefacts (Gallotti and Mussi, 2018), and Garba IVF, which yielded Oldowan lithic tools (Piperno et al., 2009).

The studied sections with their archeological levels have been placed in a virtually continuous stratigraphic framework by integrating magnetostratigraphy and $^{40}Ar/^{39}Ar$ geochronology (Morgan et al., 2012) as described in detail further below.

3. Paleomagnetism

3.1. Materials and methods

A total of 244 oriented samples distributed throughout the selected sections have been collected in 2017 by G.M. and E.M. (Fig. 2; dots to the right of the lithology logs). Samples have been obtained by inserting ~5 cm^3 plastic cylinders into unconsolidated (but still cohesive) sediments and have been oriented with a magnetic compass. Of the total samples collected,162 samples have been used for magnetostratigraphic analyses; in particular, 105 samples of the most cohesive lithologies have been extracted from the plastic cylinders by carefully cut-open the cylinders with a stainless steel blade heated to ~80 C with a heat gun, and were then subjected to thermal demagnetization from room temperature up to ~625 C in steps of 25e50 C, while 57 additional samples of less cohesive lithologies have been kept in the plastic cylinders and subjected to alternating field (AF) demagnetization in steps of 5e10 mT up to 85 mT. The natural remanent magnetization (NRM) was measured after each demagnetization step mostly with a 2G Enterprises DC-SQUID cryogenic magnetometer located in a magnetically shielded room or with a spinner magnetometer AGICO Jr-6. Magnetic component directions were extracted using least-square analysis (Kirshvink, 1980). In addition, 20 samples were subjected to backfield acquisition curves of isothermal remanent magnetization (IRM) and hysteresis experiments using a vibrating sample magnetometer Microsense EZ7, while 5 samples underwent thermal demagnetization of a three-component IRM (Lowrie, 1990) imparted in fields of 0.12 T, 0.4 T and 1.5 T using a pulse magnetizer ASC IM-10-30. Finally, 30 samples have been

stored as archive for future analyses while 27 samples, especially from GIG at Gombore, crumbled in the laboratory. Magnetic measurements were carried out at the Alpine Laboratory of Paleomagnetism (Peveragno, Italy) and the LASA Paleomagnetic
Laboratory (Segrate, Italy).

3.2. Rock magnetic analyses

Hysteresis plots of magnetization (Am^2/kg) versus applied field (Tesla, T) (representative examples in Fig. 3A; additional examples in Supplementary Figs. 1e3) were used to determine values of saturation magnetization (Ms), saturation remanence (Mr), and coercivity (Hc), after correction for the ubiquitous occurrence of paramagnetic components. The coercivity of remanence (Hcr) was determined on the same samples from IRM backfield experiments. The resulting Hc/Hcr versus Ms/Mr plot (Day et al., 1977) show that 65% of the studied samples fall in the pseudo-single domain (PSD) range of magnetite (Fig. 3B). The reminder 35% of the data falls above ranges defined for multi-domain (MD) magnetite and tend to display wasp-waisted hysteresis loops (e.g., samples GG10 and GBIV20 in Fig. 3A) suggesting the occurrence of ferromagnetic phases with contrasting coercivities (e.g. magnetite and hematite; see also below).

Thermal demagnetization experiments of a three-component IRM show a dominant signal carried by the 0.12 T curves with maximum unblocking temperatures of about 550-575 C, interpreted as due to magnetite, coexisting with a subsidiary higher coercivity component with maximum unblocking temperatures of about ~650 C, interpreted as hematite (Fig. 4). From all the above, we conclude that magnetite is the main ferromagnetic phase of the studied samples coexisting with hematite, in substantial agreement with previous findings (Tamrat et al., 2014).

3.3. Magnetostratigraphy

The NRM values of the investigated samples are well within ranges of instrumental measurability. The thermal or AF demagnetization of the NRM show the presence, in most of the samples, of a scattered initial component oriented northerly and down (normal polarity) and termed A component, removed either between room temperature and ~200 C or between 0 mT and 20 mT. A characteristic remanent magnetization (ChRM) component interpreted as representing the primary magnetic signal was isolated in 140 samples at higher temperatures, between ~200 C and 575 C, rarely up to 625 C, or higher alternating fields, from 20 mT to 80e85 mT (Fig. 5; thermal or AF demagnetization data in Supplementary Table 1). Considering also the results of the rockmagnetic experiments, the ChRM component directions appear to be carried essentially by the dominant magnetite fraction, whereas the subsidiary hematite fraction contributes very little to the ChRM (rare 'tails' above 575 C in thermal demagnetization experiments). The ChRM component directions are dipolar and oriented either downward (positive inclinations) with northerly declinations, representing normal polarity, or upward (negative inclinations) with southerly declinations, representing reverse polarity (Fig. 5). No relationships have been observed between magnetic mineralogy, which is essentially magnetite-dominated, and magnetic polarity. Standard Fisher statistics revealed that the ChRM component directions are rather scattered around a mean of Dec. ¼ 353.7E, Inc. ¼ 9.2 (k ¼ 6, a_{95}¼ 5.3, n ¼ 140) calculated by flipping reverse polarity data to normal polarity.

The values of declination and inclination of the ChRM component directions (Supplementary Table 2) were used to calculate virtual geomagnetic pole (VGP) latitudes (Supplementary Table 2) and derive magnetic polarity stratigraphy whereby positive VGP values (ideally approaching þ90) should represent normal magnetic polarity and negative values (approaching 90) reverse polarity. The maximum angular deviation (MAD) values of the ChRM component directions resulted generally lower than 20. These data have been used to delineate the magnetic polarity stratigraphy of the Melka Kunture sequence described hereafter from top to base (see Fig. 6 for data from Gombore gully, Fig. 7 for data from Garba gully, and Fig. 2 for a general overview): A clear normal magnetic polarity interval has been detected in sections GII2, upper part of G2SAG, and GX (Fig. 6) as well as in GBIII base (Fig. 7). The transition to reverse polarity occurs in section G2SAG between samples G2SAG17 and G2SAG16 (Fig. 6), as well as in correlative section GBXII between samples GBIII01 and GBIII02 (Fig. 7). Taking into account also the $^{40}Ar/^{39}Ar$ age of 0.709 ± 0.026 Ma from the Former D tuff 27e09 in section GII2 (Morgan et al., 2012), this magnetic polarity reversal is interpreted as a record of the Brunhes/Matuyama boundary
(0.773 Ma).

A consistently reverse magnetic polarity interval has been recognized in the central part of the section G2SAG and at the top of GOAMII (Fig. 6), as well as in the upper portion of GBXII (Fig. 7). A transition from reverse to normal magnetic polarity is recorded between samples G2SAG06 and G2SAG10 in section G2SAG (Fig. 6), samples GOAMII11 and GOAMII12 in section GOAMII (Fig. 6), and samples GBXIIA25 and GBXIIA26 in section GBXIIA (Fig. 7), and has been interpreted as the Matuyama/Jaramillo boundary (0.990 Ma).

A well-expressed normal polarity interval attributed to the Jaramillo Subchron has been identified in sections GOAMII and G2SAG (Fig. 6), and GBXIIA (Fig. 7), with appreciable lateral continuity. The normal-reverse polarity transition, which marks the base of the Jaramillo Subchron (1.070 Ma), lies at GOAMII between samples GOAMII16 and GOAMII03 (Fig. 6), and at GBXIIA between samples GBXIIA11 and GBXIIA13 (Fig. 7). Tuff 27e08 with an $^{40}Ar/^{39}Ar$ age of 0.875 ± 0.020 Ma (Morgan et al., 2012) should fall in Jaramillo normal polarity strata, but in section GOAMII it is located in reverse polarity strata shortly below the base of the Jaramillo (Figs. 2 and 6), and it thus

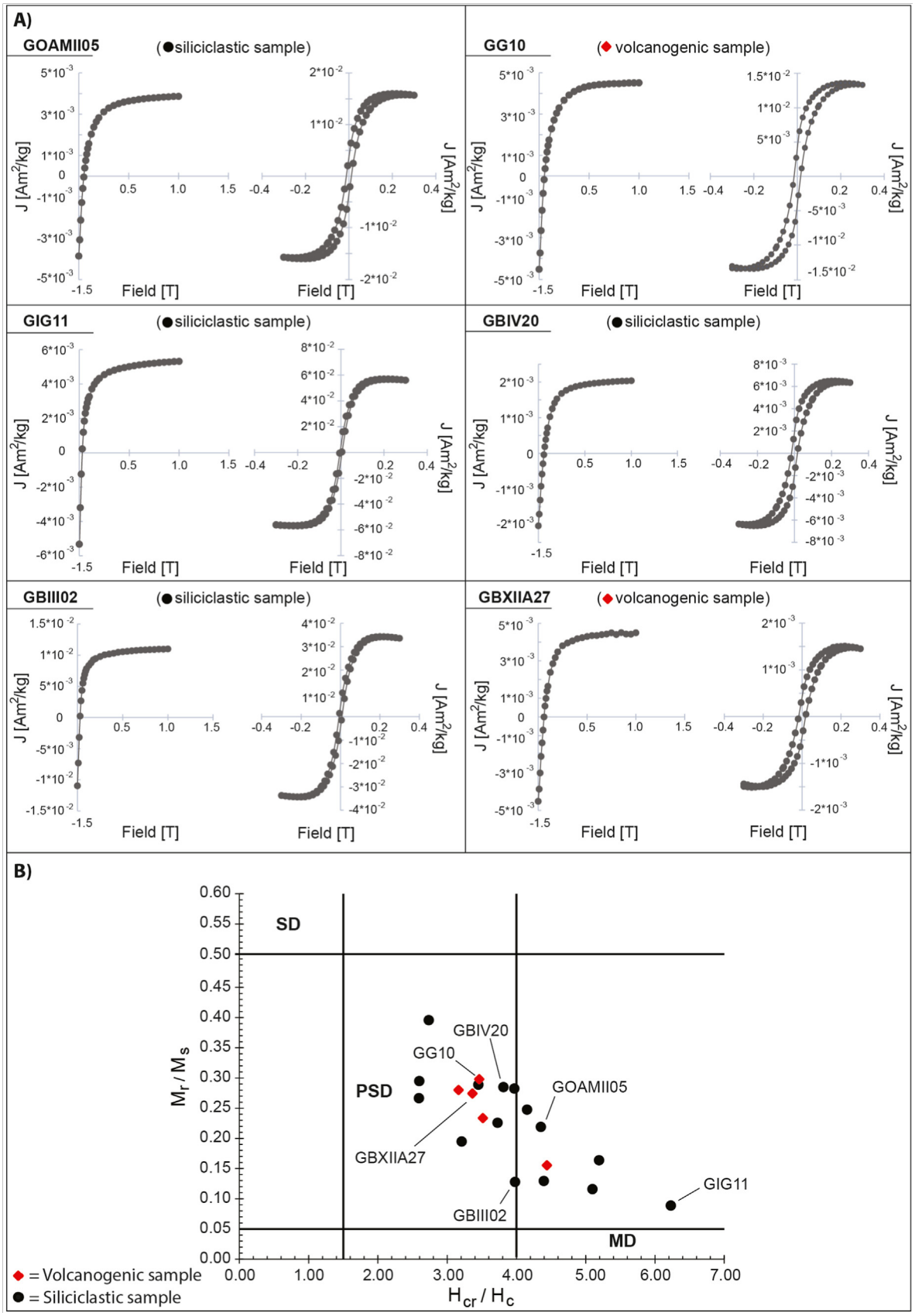
A)
GOAMII05
(●siliciclastic sample)
GG10
(◆volcanogenic sample)
GIG11
(●siliciclastic sample)
GBIV20
(●siliciclastic sample)
GBIII02
(●siliciclastic sample)
GBXIIA27
(◆volcanogenic sample)
J [Am²/kg]
Field [T]
B)
SD
PSD
MD
GBIV20
GG10
GOAMII05
GBXIIA27
GIG11
GBIII02
Mr / Ms
Hcr / Hc
◆ = Volcanogenic sample
● = Siliciclastic sample

Fig. 3. Isothermal remanent magnetization (IRM) backfield acquisition curves and hysteresis loops (corrected for paramagnetic components) have been performed on a total of 20 samples of volcanogenic and mainly siliciclastic lithologies (6 representative examples in panel A); additional examples in Supplementary Figs. 1-3). From these experiments, we extracted the values of saturation magnetization (Ms), remanent magnetization (Mr), coercivity (Hc), and coercivity of remanence (Hcr), which we plotted on the Day et al. (1977) diagram of panel B) reporting the ranges of existence of multi-domain (MD), pseudo-single domain (PSD), and single domain (SD) magnetite grains. About 65% of the analyzed

appears ~200 ky younger relative to its inferred magnetochronological age (>1.070 Ma), with important consequences on the age of the Gombore II Open Air Museum archeological site resting immediately above this level (see also further below). On this ground, the age of Tuff 27-08 has been excluded from the age model of deposition of the Gombore gully sequence as described below in Paragraph 4.

Section GII6 is characterized by reverse polarity at its top and normal polarity at its base, with the polarity transition situated between samples GII604 and GII605 (Fig. 6). This thin normal polarity interval is a possible record of the Cobb Mountain Subchron (1.180e1.210 Ma). A similar polarity excursion has been detected also in sections GIISag 2017I and GXIS (samples GIIS17I11, GIIS17I09, and GXIS27; Fig. 6).

Proceeding down-section, a clear reverse polarity interval interpreted as a record of the (pre-Cobb Mountain?) Matuyama characterizes sections GXIS, GIISag17, as well as GG, GIG and GIS (Fig. 6), although several samples from these sections e especially GIG e could not be analyzed for magnetostratigraphy as they crumbled in the laboratory.

Section GBIVO (Fig. 7) shows a clear normal polarity signal which has been interpreted as a partial record of the Olduvai Subchron. The transition from normal to reverse polarity observed between samples GBIV07 and GBIVO04 (Fig. 7) should therefore correspond to the Olduvai/Matuyama boundary (1.925 Ma).

Mainly reverse polarity characterizes the central-lower portion of section GBIV (Fig. 7). Tuff 27e23 "Grazia" with a mean $^{40}Ar/^{39}Ar$ age of 1.719 Ma (and large analytical errors of ±0.398 Ma at 2s; Morgan et al., 2012) should fall above or within Olduvai normal polarity strata, but in section GBIV it is located in reverse polarity strata shortly below the base of the Olduvai (Figs. 2 and 7), and it thus appears some ~200 ky younger relative to its inferred magnetochronological age (>1.925 Ma). On this ground, the age of Tuff 27e23 "Grazia" has been excluded from the age model of deposition of the Garba gully sequence described below in Paragraph 4. Finally, the base of section GBIV contains two superposed samples of normal magnetic polarity, with the reverse-normal polarity transition placed between samples GBIV10 and GBIV13 (Fig. 7). We tentatively interpret this lowermost normal polarity interval as a partial record of the Reunion Subchron (2.116e2.137 Ma), albeit we acknowledge the overall complexity of the VGP polarity pattern in section GBIV (Fig. 7).

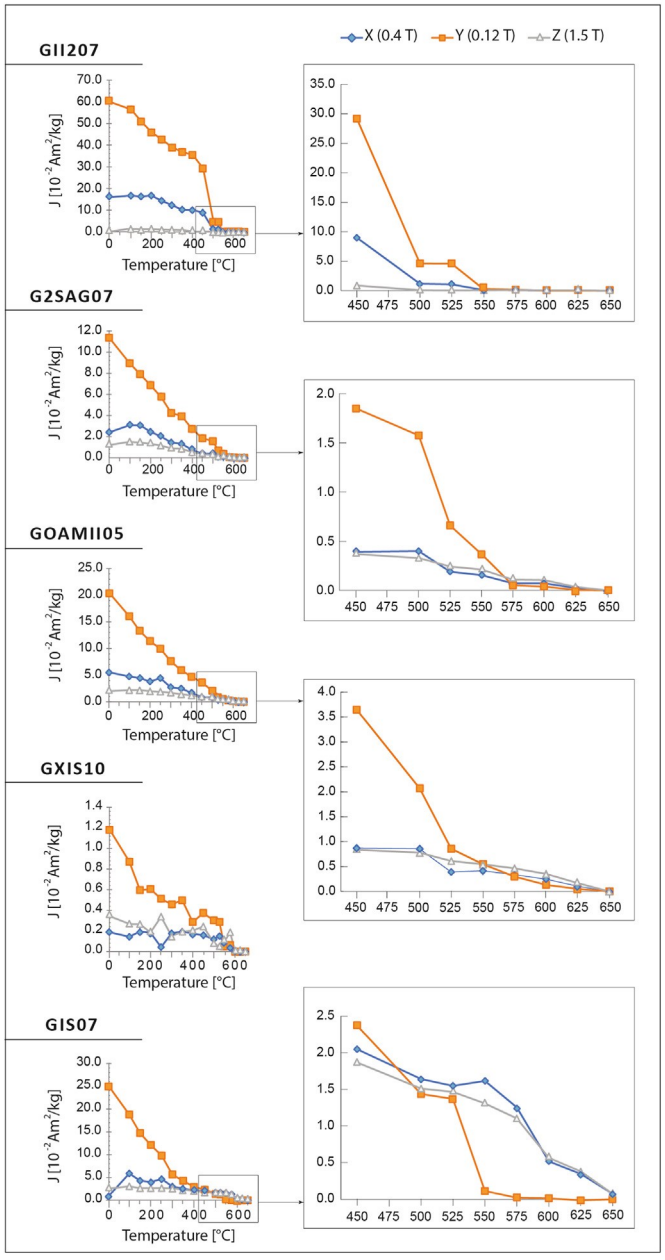

Fig. 4. Thermal decay of a three-component IRM (acquired in 1.5 T, 0.4 T, and 0.12 T fields) of selected samples of volcanogenic and mainly siliciclastic lithologies. Exploded-view panels on the right illustrate the existence in the studied samples of a magnetite phase with maximum unblocking temperatures of 550e575 C variably coexisting with a magnetic phase with maximum unblocking temperature of 650 C interpreted as hematite. The wasp-waisted shapes of some of the studied samples (Fig. 3) confirm the occurrence of a mixed-coercivity magnetic mineralogy.

4. Age models of sedimentation

In an attempt to establish best-fit age models of sedimentation of the Melka Kunture succession, two virtually continuous stratigraphies have been reconstructed, one for Gombore gully and the other for Garba gully, by piecing together in a common metric scale the constituent stratigraphic sections according to the correlation scheme of Fig. 2. Onto these continuous stratigraphies, we placed key age-depth tie points for sedimentation rate modelling, as described hereafter.

The age model for Gombore gully has been constructed by adopting seven age-depth tie-points represented by (i) the Brunhes/Matuyama boundary (0.773 Ma), (ii) top Jaramillo (0.990 Ma), (iii) base Jaramillo (1.070 Ma), (iv) top Cobb Mountain (1.180 Ma), as well as the $^{40}Ar/^{39}Ar$ ages of (v) Former D tuff 27e09 (0.709 ± 0.026 Ma), (vi) Former B Tuff 27e12 (1.200 ± 0.140 Ma), and (vii) Tuff 27e03 (1.393 ± 0.324 Ma) from Morgan et al. (2012; with errors at 2s level) (Fig. 8A; see also Supplementary Table 3). Similarly, the age model

for Garba has been constructed by adopting five recorded chronologic tie-points: (i) the Brunhes/

samples fall in the PSD range while the reminder of the samples fall above the MD range, reflecting the existence of a complex mineralogy with contrasting coercivities, as reflected also by the wasp-waisted shapes of the corresponding hysteresis loops (e.g., sample GOAMII05).

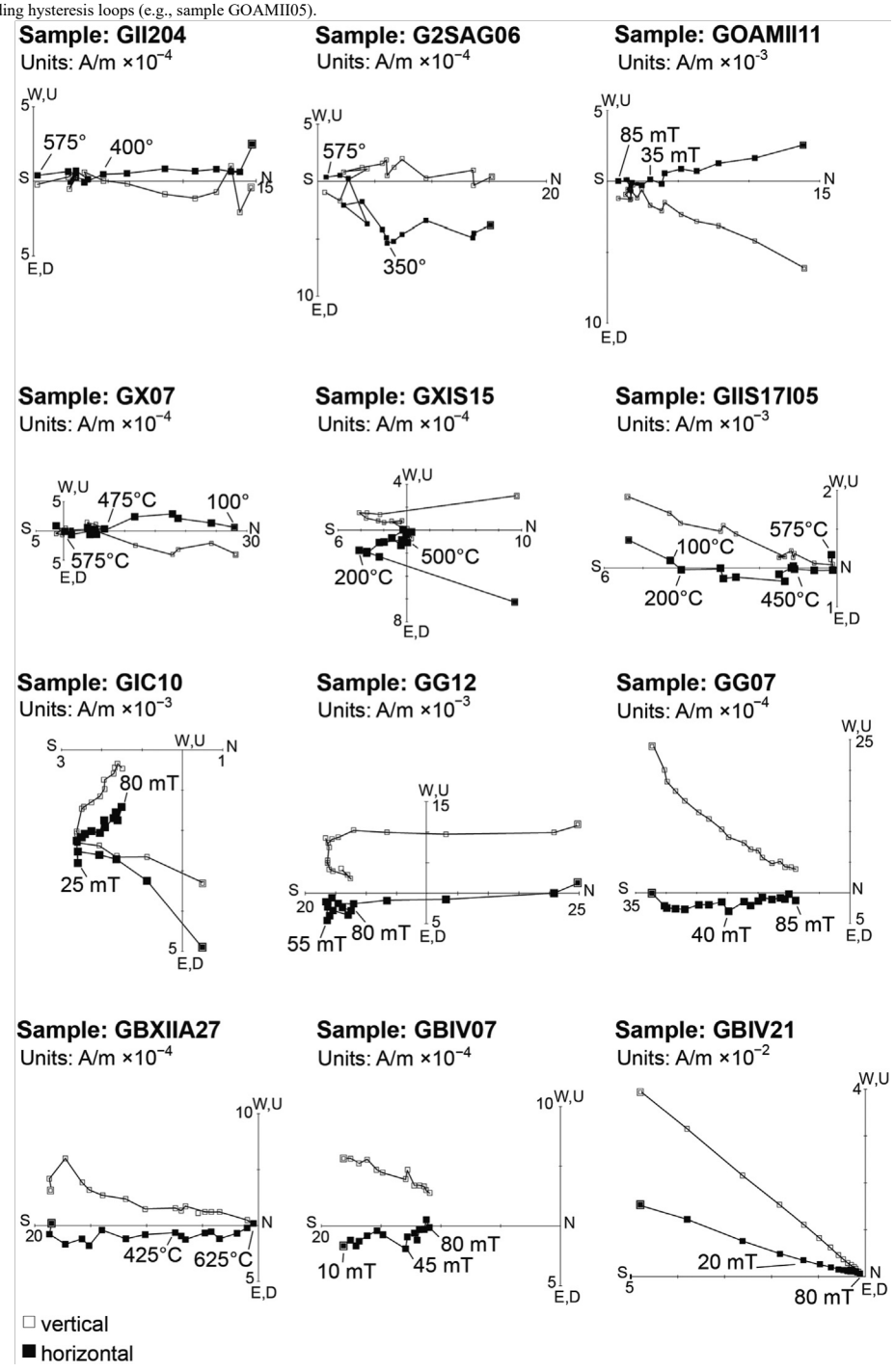

Fig. 5. Vector end-point demagnetization diagrams of representative samples showing the presence of northerly-and-down or southerly-and-up characteristic remanent magnetization component (ChRM) directions indicating respectively normal or reverse polarity. Transitional directions are observed in some cases (e.g., sample GIC10). Closed symbols are projections onto the horizontal plane and open symbols onto the vertical plane in geographic (in situ) coordinates (equivalent to tilt-corrected coordinates as bedding is essentially horizontal). Demagnetization steps are expressed in C or mT.

Matuyama boundary (0.773 Ma), (ii) top Jaramillo (0.990 Ma), (iii) base Jaramillo (1.070 Ma), (iv) base Olduvai (1.925 Ma), and (v) top Reunion (2.116 Ma) (Fig. 8B; see also Supplementary Table 3). As stated above, we excluded

from the inventory of tie-points the $^{40}Ar/^{39}Ar$ ages of Tuff 27e08 from Gombore and Tuff 27e23 "Grazia" from Garba because they are in contradiction relative to the

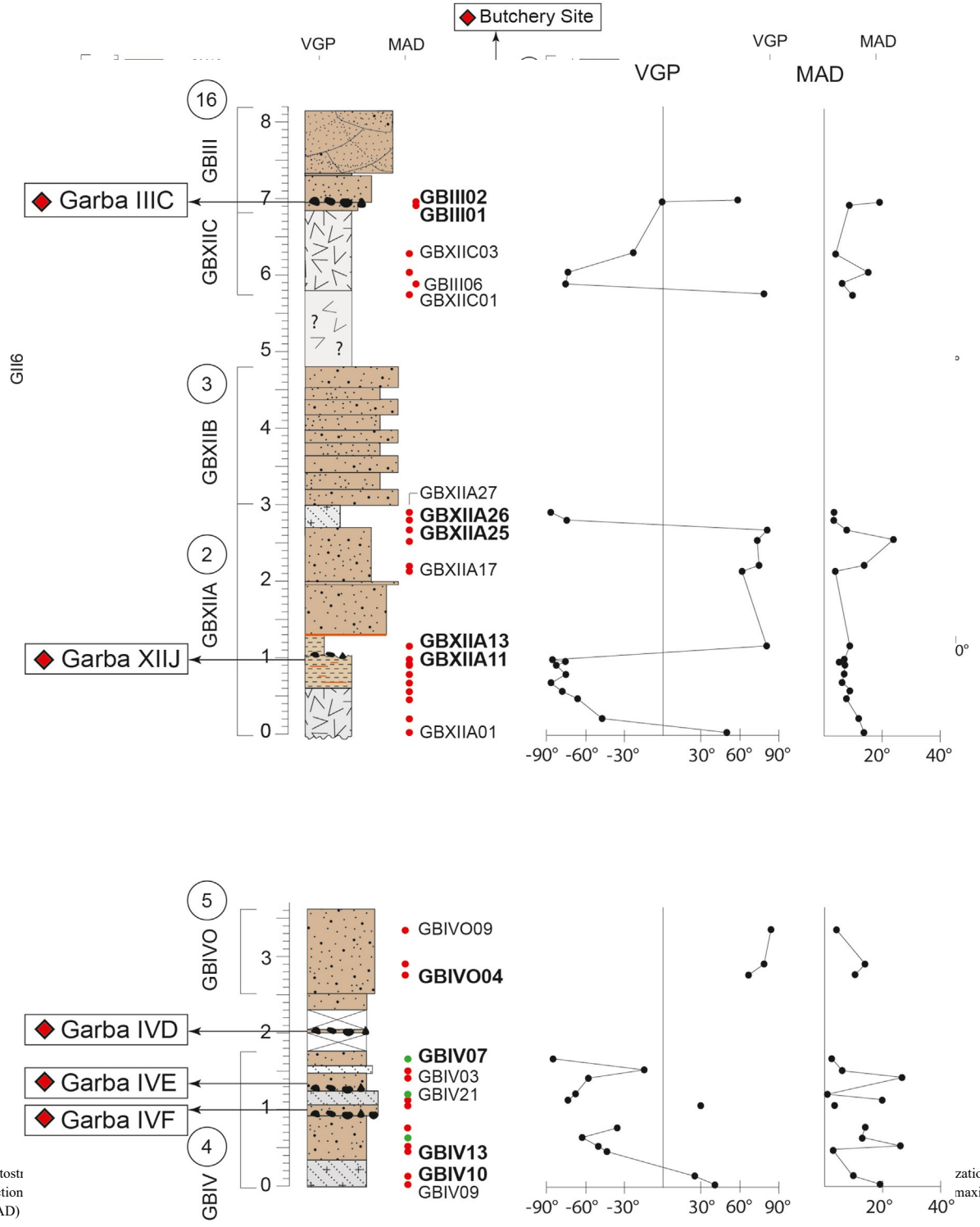

Fig. 6. Magnetostr
(ChRM) direction
deviation (MAD)

zation component
maximum angular

Fig. 7. Magnetostratigraphic data of Garba gully lithostratigraphic sections. Symbols and parameters as in Fig. 6. See also Fig. 2 and text for discussion.

overall magnetostratigraphy of the levels in which they are found (see above). Best-fit interpolations of these chronologic tie-points with associated envelopes of 95% confidence have been obtained using software PAST (Hammer et al., 2001).

For Gombore gully, we generated a simple linear age model of deposition that takes the form of Depth(m) ¼ 18.6*Age(Ma) þ 32.6 (correlation coefficient r^2 ¼ 0.93), where Depth(m) represents the depth in meters of the composite stratigraphy and Age (Ma) the corresponding age in Ma. The average sedimentation rate, represented by the slope of the best-fit line, is thus of 18.6 m/Ma (Fig. 8A). The basal part

of the Gombore gully composite sequence, lacking direct magnetochronological and/or geochronological constraints, was tentatively dated by linear extrapolation of the best-fit line (dashed line in Fig. 8A). Incidentally, this part of the sequence contains (undated) Tuff 9947 "Graziella" in section GIC (Fig. 2) that Raynal and Kieffer (2004) correlated using geochemistry to Tuff 27e23 "Grazia"

(1.719 ± 0.398 Ma) from section GBIV (but see above about the

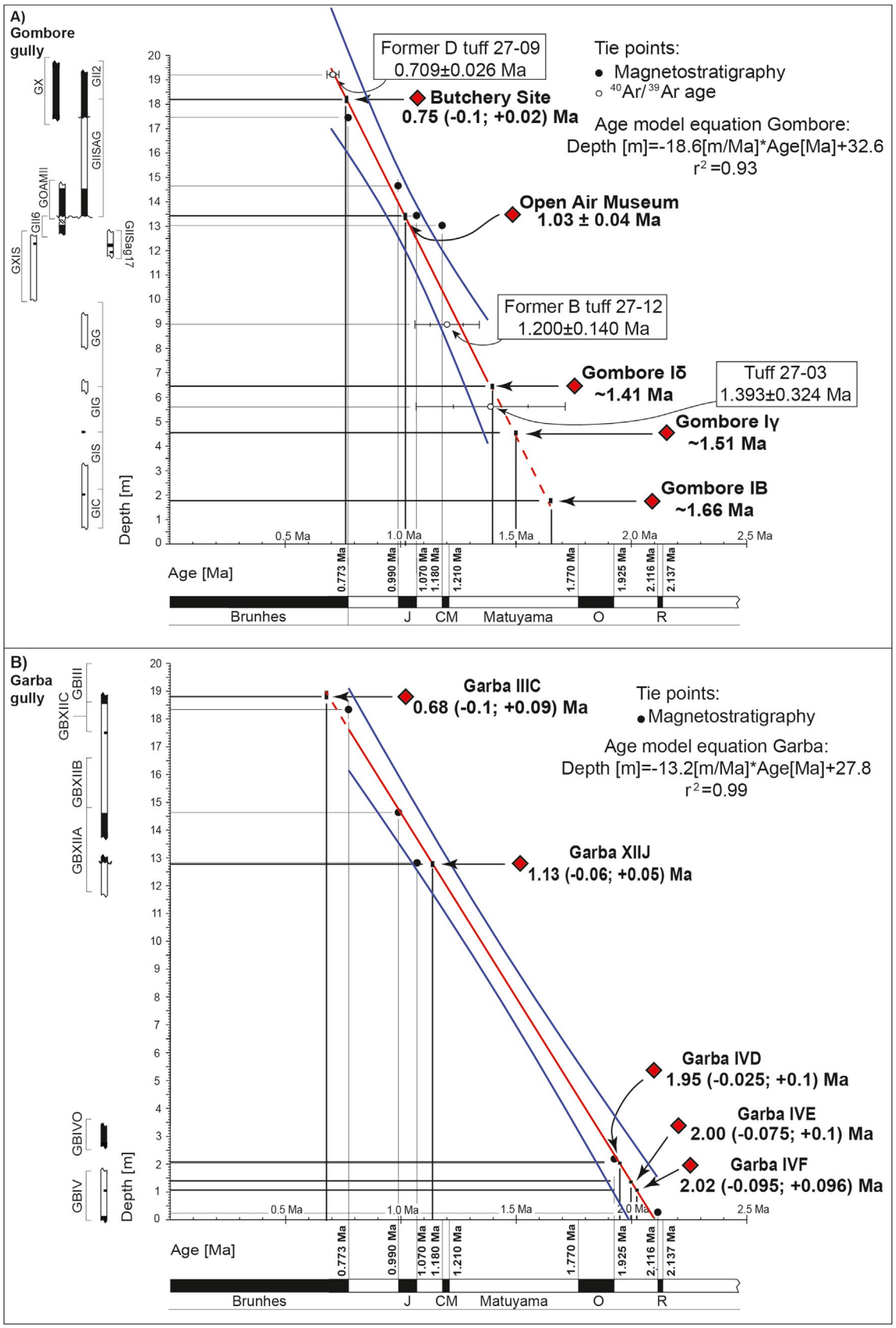

Fig. 8. Composite stratigraphic sequences of Gombore gully (A) and Garba gully (B), in meters from base, correlated to the geomagnetic polarity time scale of Channell et al. (2020) using magnetochronologic and radiometric tie-points (Supplementary Table 3) fitted by simple linear regression models with associated envelopes of 95% confidence. These linear age models of sedimentation

are used to derive interpolated or extrapolated mean ages and associated ± errors of the main archeological levels present at Gombore gully and Garba gully (ages reported in bold in figure). J is Jaramillo Subchron, CM is Cobb Mountain Subchron, O is Olduvai Subchron, and R is Reunion Subchron. See text for discussion.

reliability of this datum). We found that several other tuffs present throughout the Melka Kunture sequence share similar compositions (see details in Supplementary Figs. 4 and 5), and hence we consider geochemistry hardly diagnostic for correlating and dating of the basal part of the Gombore sequence. Regarding the Garba sequence, the linear best-fit age model (and associated envelope of 95% confidence) that interpolates the selected chronologic tiepoints takes the form of Depth(m) ¼ 13.2*Age(Ma) þ 27.8 (correlation coefficient r^2 ¼ 0.99), implying an average sediment accumulation rate of 13.2 m/Ma (Fig. 8B) that is slightly lower than at Gombore (18.6 m/Ma) because of the lateral variability in thickness of the investigated sedimentary bodies.

We tested also alternative and more complex age models, including models based on second-order polynomials, which, although sometimes producing high correlation indexes, often violated the magnetic polarity recognized throughout the stratigraphy, and have therefore been discarded. We stress that the linear age models we applied, with outstanding correlation coefficients of r^2 ¼ 0.93 for Gombore gully and r^2 ¼ 0.99 for Garba gully, are in their simplicity very robust, and provide interpolated ages that do not violate the magnetochronological constraints used for the construction of the models (Fig. 8). In any case, alternative age models can be constructed by using data in Supplementary Table 3. 5. Inferred ages of the main archeological levels

The linear best-fit age models described above have been used to assess the ages of the main archeological levels at Gombore gully (Fig. 8A) and Garba gully (Fig. 8B), as described hereafter (see also Fig. 2). The ± errors attached to the mean ages have been derived from the 95% confidence intervals of the best-fit lines, and are therefore symmetrical, but in some cases it was necessary to truncate them on the positive (þ) and/or negative (-) side in order to avoid violating the magnetochronology; for example, the mean age of a level of reverse polarity cannot embrace with its ± error bar normal polarity levels located below and/or above it, and hence the error bar must be truncated at the appropriate age allowed by the magnetochronology, producing asymmetrical errors. The following ages of archeological levels have been derived: The extrapolated mean ages of the archeological levels Gombore II Butchery site (Fig. 8A) and Garba IIIC (Acheulean level) (Fig. 8B), both located in the early Brunhes Chron, are of 0.75 (0.1; þ0.02) Ma and 0.68 (0.1; þ0.09) Ma, respectively. The interpolated mean age of the archeological level Gombore II Open Air Museum is of 1.03 (±0.04) Ma (Fig. 8A). In particular, this level, represented by a basal fluvial lag deposit (stoneline), is of normal (Jaramillo) magnetic polarity, while the tuff level immediately below the base of the lag deposit is of reverse (Matuyama) polarity, and hence the base of the stoneline falls at the Jaramillo/Matuyama boundary at a nominal age of 1.070 Ma. As stated above, the $^{40}Ar/^{39}Ar$ age of tuff level 27e08, located immediately below the stoneline in reverse polarity (pre-Jaramillo) sediments, appears ~200 ky younger than its inferred magnetochronological age (and has been excluded from age modelling).

The age of the Garba XIIJ archeological site (Fig. 8B), which lies in reverse polarity sediments immediately below the base of the Jaramillo/Matuyama boundary (1.070 Ma), is estimated at 1.13 (0.06; þ0.05) Ma.

The extrapolated ages of ~1.41 Ma, ~1.51 Ma and ~1.66 Ma for archeological levels Gombore Id, Gombore Ig and Gombore IB (Fig. 8A), respectively, should be taken with caution, lacking the basal Gombore sequence of robust direct chronological constraints.

The mean ages of the Garba IV archeological levels (Fig. 8B), magnetostratigraphically comprised between the base of the Olduvai Subchron and the top of the (inferred) Reunion Subchron, resulted of 1.95 (0.025; þ0.1) Ma for Garba IVD, 2.00 (0.0075; þ0.1) Ma for Garba IVE, and 2.02 (0.095; þ0.096) Ma for Garba IVF (Fig. 8B).

6. Conclusions

We identified the stratigraphic positions of the main polarity reversals of the Earth's magnetic field in the Melka Kunture sedimentary succession at the Gombore and Garba gullies. The new magnetostratigraphic data allowed us to contribute dating the several archeological levels therein contained that are of exceptional relevance for understanding the patterns of human evolution in Africa during the Pleistocene. Rock magnetic analyses indicate that the main magnetic mineral that carries the primary magnetostratigraphic signal is magnetite, mostly in the pseudo-single domain range, variably associated with a higher coercivity hematite fraction. Magnetochronological tie-points (e.g., Brunhes/ Matuyama boundary, top Jaramillo, base Jaramillo, base Olduvai, etc.; ages after Channell et al., 2020) derived from the reconstructed magnetic polarity pattern have been used in conjunction with a critical selection of $^{40}Ar/^{39}Ar$ ages from the literature (Morgan et al., 2012) to build accurate e and simple e age models of sedimentation for the Melka Kunture sequence from which we derived the mean age estimates of the main levels of archeological significance, from Garba IIIC with Acheulean lithic industry at 0.68 (0.1; þ0.09) Ma to Garba IVF with Oldowan tools at 2.02 (0.095; þ0.096) Ma. From these analyses, it appears that the Melka Kunture succession covers in relatively stratigraphic continuity a time interval spanning from the Brunhes Chron at the top to the Reunion Subchron at the base, or from ~0.6 to ~2.1 Ma. More problematic resulted the age assessments of archeological levels Gombore Id, Gombore Ig and Gombore IB because of extensive gaps in the magnetostratigraphic record and absence of direct geochronologic dating of tuff levels in the lower part of the Gombore sequence. Future work will involve filling-in the lower Gombore magnetostratigraphic gap and attempt dating critical tuff 9947 "Graziella" at Gombore I as well as redating Tuff 27e23 ''Grazia'' at Garba IV.

Credit author statement

Serena Perini: Data analyses, Conceptualization, Manuscript writing and figures preparation. Giovanni Muttoni: Conceptualization, Data curation, Field-work and sampling, Manuscript writing. Edoardo Monesi: Field-work and sampling, Data analyses. Rita Melis: Supervision. Margherita Mussi: Supervision.

Declaration of competing interest

The authors declare that they have no known competing financial interests or personal relationships that could have appeared to influence the work reported in this paper.

Acknowledgements

We would like to thank Giuseppe Lembo for total station data used to construct Fig. 1, and Rosalia Gallotti for help in the field and insightful discussions. Giovanni Muttoni would like to thank the Rector of the Universita degli Studi di Milano for fundings and support. The Italian Archeological Mission at Melka Kunture was funded in 2017 by Universita di Roma La Sapienza (Grandi Scavi- grant SA11715C7C936C01) and by Ministero degli Affari Esteri e della Cooperazione Internazionale (grant ARC-001666). The

research permits where provided by the Authority for Research and Conservation of the Cultural Heritage which also helped in many ways, together with the authorities of the Oromyia Federal
Republic.

Appendix A. Supplementary data

Supplementary data to this article can be found online at https://doi.org/10.1016/j.quascirev.2021.107259.

References

Altamura, F., Gaudzinski-Windheuser, S., Melis, R.T., Mussi, M., 2020. Reassessing hominin skills at an early middle Pleistocene hippo Butchery site: Gombore II-2 (Melka kunture, upper Awash Valley, Ethiopia), 2020 J. Paleolit. Archaeol. 3, 1e32. https://doi.org/10.1007/s41982-019-00046-0.

Bardin, G., Raynal, J.P., Kieffer, G., 2004. Drainage pattern and regional morphostructure at Melka kunture (upper Awash, Ethiopia). In: Chavaillon, J., Piperno, M. (Eds.), 2004. Studies on the Early Paleolithic site of Melka Kunture, Ethiopia. Origines, Istituto Italiano di Preistoria e Protostoria, pp. 83e92. Florence.

Channell, J.E.T., Singer, B.S., Jicha, B.R., 2020. Timing of Quaternary geomagnetic reversals and excursions in volcanic and sedimentary archives. Quat. Sci. Rev. https://doi.org/10.1016/j.quascirev.2019.106114.

Chavaillon, J., 1979. Stratigraphie du site archeologique de Melka-Kunture (Ethiopie). Bull. Soc. Geol. Fr. 7 (I), 227e232. XXI, n3.

Chavaillon, J., Coppens, Y., 1986. Nouvelle decouverte d'Homo erectus a MelkaKunture. Comptes Rendus l'Acad. Sci. Paris 303 (II), 99e104.

Chavaillon, J., Piperno, M., 2004. Studies on the Early Paleolithic Site of Melka Kunture, Ethiopia, Origines, Istituto Italiano di Preistoria e Protostoria. Florence. Chavaillon, J., Berthelet, A., 2004. The archaeological sites of Melka Kunture. In: Chavaillon, J., Piperno, M. (Eds.), Studies on the Early Paleolithic site of Melka Kunture, Ethiopia. Istituto Italiano di Preistoria e Protostoria, Florence, pp. 25e80.

Chavaillon, J., Brahimi, C., Coppens, Y., 1974. Premiere decouverte d'Hominide dans l'un des sites acheuleens de Melka-Kunture (Ethiopie). Comptes Rendus l'Acad. Sci. Paris 278, 3299e3302.

Chavaillon, J., Chavaillon, N., Hours, F., Piperno, M., 1979. From the Oldowan to the Middle Stone Age at Melka-Kunture (Ethiopia). Understanding cultural changes. Quat. Storia Nat. Cult. Quat. Roma 21, 87e114, 1979.

Condemi, S., 2004. The Garba IV E mandible. In: Chavaillon, J., Piperno, M. (Eds.), Studies of the Early Paleolithic site of Melka Kunture, Ethiopia. Istituto Italiano di Preistoria e Protostoria, Florence, pp. 687e701.

Day, R., Fuller, M., Schmidt, V.A., 1977. Hysteresis properties of titanomagnetites: grain-size and compositional dependence. Phys. Earth Planet. In. 13 (4), 260e267. https://doi.org/10.1016/0031-9201(77)90108-X.

Di Vincenzo, F., Rodriguez, L., Carretero, J.M., Collina, C., Geraads, D., Piperno, M., Manzi, G., 2015. The massive fossil humerus from the oldowan horizon of Gombore I, Melka kunture (Ethiopia, >1.39 Ma). Quat. Sci. Rev. 122, 207e221.

Gallotti, R., 2013. An older origin for the acheulean at Melka kunture (upper Awash, Ethiopia): techno-economic behaviours at Garba IVD. J. Hum. Evol. 65 (5), 594e620. https://doi.org/10.1016/j.jhevol.2013.07.001.

Gallotti, R., Mussi, M., 2017. Two acheuleans, two humankinds: from 1.5 to 0.85 Ma at Melka kunture (upper Awash, Ethiopian highlands). J. Anthropol. Sci. 95, 1e46.

Gallotti, R., Mussi, M., 2018. Before, During, and After the Early Acheulean at Melka Kunture (upper Awash, Ethiopia): A Techno-economic Comparative Analysis. In: Gallotti, R., Mussi, M. (Eds.), The Emergence of the Acheulean in East Africa and Beyond, Contributions in Honor of Jean Chavaillon. Springer, pp. 53e92.

Gallotti, R., Collina, C., Raynal, J.-P., Kieffer, G., Geraads, D., Piperno, M., 2010. The early Middle Pleistocene site of Gombore II (Melka Kunture, upper Awash, Ethiopia) and the issue of Acheulean bifacial shaping strategies. Afr. Archaeol. Rev. 27, 291e322.

Hammer, Ø., Harper, D.A.T., Ryan, P.D., 2001. Past: paleontological statistics software package for education and data analysis. Palaeontol. Electron. 4 (1) art. 4: 9pp.

Kieffer, G., Raynal, J.P., Bardin, G., 2002. Cadre structural et volcanologique des sites du Paleolithique ancient de Melka Kunture (Awash, Ethiopie): premiers resultats, vol. 2. Les Dossiers de l'Archeologie n, Goudet, France, pp. 77e92.

Kieffer, G., Raynal, J.P., Bardin, G., 2004. Volcanic markers in coarse alluvium at Melka kunture (upper Awash, Ethiopia). In: Chavaillon, J., Piperno, M. (Eds.), 2004. Studies on the Early Paleolithic site of Melka Kunture, Etiopia. Origines, Istituto Italiano di Preistoria e Protostoria, pp. 93e101. Florence.

Kirshvink, J.L., 1980. The least-squares line and plane and the analysis of palaeomagnetic data. Geophys. J. Int. 62, 699e718. https://doi.org/10.1111/j.1365246X.1980.tb02601.x.

Lowrie, W., 1990. Identification of ferromagnetic minerals in a rock by coercivity and unblocking temperature properties. Geophys. Res. Lett. 17 (2), 159e162.

Mendez-Quintas, E., Panera, J., Altamura, F., Di Bianco, L., Melis, R.T., Piarulli, F., Ruta, G., Mussi, M., 2019. Gombore II (Melka Kunture, Ethiopia): a new approach to formation processes and spatial patterns of an Early Pleistocene
Acheulean site. J. Archaeol. Sci. 108, 104975. https://doi.org/10.1016/j.jas.2019.104975.

Morgan, L.E., Renne, P.R., Kieffer, G., Piperno, M., Gallotti, R., Raynal, J.-P., 2012. A chronological framework for a long and persistent archaeological record: Melka Kunture, Ethiopia. J. Hum. Evol. 62, 104e115.

Mussi, M., Altamura, F., Macchiarelli, R., Melis, R.T., Spinapolice, E.E., 2014. Garba III (Melka Kunture Ethiopia): a Middle stone age site with archaic Homo sapiens remains revisited. Quat. Int. 343, 28e39.

Mussi, M., Altamura, F., Bonnefille, R., De Rita, D., Melis, R.T., 2016. The environment of the Ethiopian highlands at the Mid Pleistocene Transition: fauna, flora and hominins in the 850-700ka sequence of Gombore II (Melka Kunture). Quat. Sci. Rev. 149, 259e268.

Mussi, M., Altamura, F., Di Bianco, L., Bonnefille, R., Gaudzinski-Windheuser, S., Geraads, D., Melis, R.T., Panera, J., Piarulli, F., Pioli, L., Ruta, G., Sanchez-Dehesa Galan, S., M endez-Quintas, E., 2021. After the emergence of the acheulean at Melka kunture (upper Awash, Ethiopia): from Gombore IB (1.6 Ma) to Gombore Ig (1.4 Ma), Gombore Id (1.3 Ma) and Gombore II OAM test pit C (1.2 Ma). Quat.
Int. https://doi.org/10.1016/j.quaint.2021.02.031.

Mussi, M., Gallotti, R., 2014. The Emergence of the Acheulean in East Africa e International Workshop, Rome, "La Sapienza" University, September 12e13, 2013. Evol. Anthropol. 23 (4), 126e127.

Piperno, M., 2001. The prehistory of Melka kunture (Ethiopia). Bull. Cent. Rech. Fr. Jerusalem 8, 135e145.

Piperno, M., Collina, C., Gallotti, R., Raynal, J.-P., Kieffer, G., le Bourdonnec, F.-X., Poupeau, G., Geraads, D., 2009. Obsidian exploitation and utilization during the Oldowan at Melka Kunture (Ethiopia). In: Interdisciplinary Approaches to the Oldowan. Vertebrate Paleobiology and Paleoanthropology. Springer, Dordrecht, pp. 111e128.

Profico, A., Di Vincenzo, F., Gagliardi, L., Piperno, M., Manzi, G., 2016. Filling the gap. Human cranial remains from Gombore II (Melka Kunture, Ethiopia; ca. 850 ka) and the origin of Homo heidelbergensis. J. Anthropol. Sci. 94, 1e24. https:// doi.org/10.4436/jass.94019.

Raynal, J.P., Kieffer, G., 2004. Lithology, dynamism and volcanic successions at Melka Kunture (upper Awash, Ethiopia). In: Chavaillon, J., Piperno, M. (Eds.), Studies on the Early Paleolithic Site of Melka Kunture, Ethiopia, Origines, Istituto Italiano di Preistoria e Protostoria, pp. 115e135. Florence.

Raynal, J.P., Kieffer, G., Bardin, G., 2004. Garba IV and the Melka Kunture formation. A preliminary lithostratigraphic approach. In: Chavaillon, J., Piperno, M. (Eds.), Studies on the Early Paleolithic Site of Melka Kunture, Ethiopia, Origines, Istituto Italiano di Preistoria e Protostoria, pp. 137e166. Florence.

Royer, P., Coppens, Y., 1975. Decouverte d'hominid e dans un site acheul een de Melka-Kunture (Ethiopie). Bull. Mem. Soc. Anthropol. Paris Ser. XIII 2 (2), 125e128. https://doi.org/10.3406/bmsap.1975.1807.

Schmitt, J.J., Wempler, J.M., Chavaillon, J., Andrews, M.C., 1977. Initial K-Ar and paleomagnetic results of the Melka Kunture early-man sites, Ethiopia. In: Proceedings VIII Panafrican Congress of Prehistory and Quaternary Studies. Nairobi.

Tamrat, E., Thouveny, N., Taieb, M., Brugal, J.P., 2014. Magnetostratigraphic study of the Melka Kunture archaeological site (Ethiopia) and its chronological implications. Quat. Int. 343, 5e16.

Westphal, M., Chavaillon, J., Jaeger, J.J., 1979. Magnetostratigraphie des dep o^ts Pleistocenes de Melka-Kunture (Ethiopie): premieres donnees. Bull. Soc. Geol. Fr. 7, 237e241.

Zanolli, C., Dean, M.C., Assefa, Y., Bayle, P., Braga, J., Condemi, S., Endalamaw, M., Redae, B.E., Macchiarelli, R., 2017. Structural organization and tooth development in a Homo aff. erectus juvenile mandible from the Early Pleistocene site of Garba IV at Melka Kunture, Ethiopian highlands, 2016 Am. J. Phys. Anthropol. 162, 533e549. https://doi.org/10.1002/ajpa.23135.

Zilberman, U., Smith, P., Condemi, S., 2004a. Evidence for a genetic disorder affecting tooth formation in the Garva IV child. In: Chavaillon, J., Piperno, M. (Eds.), Studies on the Early Paleolithic site of Melka Kunture, Ethiopia. Istituto Italiano di Preistoria e Protostoria, Florence, pp. 703e713.

Zilberman, U., Smith, P., Piperno, M., Condemi, S., 2004. Evidence of amelogenesis imperfecta in an early African Homo erectus. J. Hum. Evol. 46 (6), 647e653. https://doi.org/10.1016/j.jhevol.2004.02.005.